PROGRESS IN COLOR, COLORANTS AND COATINGS

available online @ www.pccc.icrc.ac.ir

Progress in Color Colorants Coating 18 (2025), 479-491

Ministry of Science, Research and Technology
Institute for Color Science & Technology

Synthesis of Zinc Oxide Nanocatalyst Via Hydrothermal Method for Photocatalytic Oxidation Process of Refinery Wastewater

L. T. Hadi[1], R. T. Al-khateeb[2], A. A. Hassan[*2,3]

[1.] Department of ICT, AL-Furat Al-Awsat Technical University, P.O. Box: 54001, Muthanna, Iraq
[2.] Department of Chemical Engineering, University of Muthanna, P.O. Box: 1550, Muthanna, Iraq
[3.] College of Engineering, Al Ayen University, P.O. Box: 64001, Nasiriyah, Iraq

ARTICLE INFO

Article history:
Received: 04 Mar 2025
Final Revised: 18 May 2025
Accepted: 26 May 2025
Available online: 30 July 2025

Keywords:
Refinery wastewater
Water treatment
Advanced oxidation process
Photo-catalytic

ABSTRACT

The increasing environmental concerns due to industrial wastewater, particularly from refineries, necessitate the development of efficient and sustainable wastewater treatment methods. In this study, zinc oxide (ZnO) nanocatalysts were synthesized via a simple and cost-effective hydrothermal method for their application in the photocatalytic oxidation process to degrade organic contaminants in refinery wastewater. The hydrothermal synthesis conditions, including temperature, precursor concentration, and reaction time, were optimized to achieve high-quality ZnO nanostructures with enhanced photocatalytic activity. The structural, morphological, and optical properties of the synthesized ZnO were characterized using techniques such as X-ray XRD, FE-SEM, FTIR, DRS, and UV-Vis spectroscopy. The organic removal reached 93.89 % and 91.28 % at best conditions of 9 pH, 0.25 Nano catalyst dose, and 120 min irradiation time of prepared nano zinc oxide and commercial titanium dioxide with UV light respectively. The aptitude of the catalyst dose to eliminate organic content was amplified after the addition of different amounts of agents. Usually, photocatalytic oxidation is meaningful through its high aptitude in the direction of oxide organic compounds in refinery wastewater. Prog. Color Colorants Coat. 18 (2025), 479-491© Institute for Color Science and Technology.

1. Introduction

The regular growths of oil and gas manufacturing include an enormous quantity of injected water toward affluence and the retrieval of oil [1]. This water remains on cloud nine to the surface along with pollutants material, salt, and added solutes, and is frequently recognized by way of “oily wastewater" [2, 3], and diverse from one oilfield to another owing to the difference in the kind of oil produced [4]. These wastewaters are multi-layered and include many organic and inorganic materials, for instance, oil dissolved, sulfur, and many dangerous materials byproducts [5, 6], and vary in concentration amid wells and over the lifetime of a healthy. Because all organic matter cannot be dissolved by water, the majority of these chemicals end up being scattered within it [7, 8]. Then are eliminated either directly or indirectly from the environ-ment, completing the water, air, and food sources [9]. These discharges are not recyclable and might knowledge changes that have enormous environmental, public health, and financial influences [10].

These materials are problematic for luxury owing to high concentrations of pollutants in refinery wastewater [11, 12]. The treatment of refinery wastewater is important through reason of lawmaking and ecological anxieties. Altogether lengthways extra severe ecological rules essential varied refinery wastewater action

*Corresponding author: * ali.alkhafaji@mu.edu.iq
https://doi.org/10.30509/pccc.2025. 167484.1368

from oil and gas productions previously released and before immunization into reservoirs toward reduction creation damage.Currently, correctly treated water can be secondhand and rummage-sale aimed at water flooding. This stage can involve the advanced oxidation processes (AOPs) request, which are optional when components of refinery wastewater have a high biochemical constancy and/or low biodegradability [13]. The treatment of wastewater utilizing AOPs can crop the comprehensive mineralization of pollutants to water, CO_2, and inorganic materials [14]. AOPs can remain intimate in two groups: Non-photochemical and Photochemical. Non-photo-chemicals include Fenton, ozonation, and ozone/ hydrogen peroxide [15].

The photochemical oxidation procedures comprise photochemical with UV lamp and heterogeneous (photocatalysis, etc.) processes [16]. Photocatalytic squalor is one of the many active oxygen producers (AOPs). ZnO, TiO_2, or CdS are possible catalysts in sophisticated chemical processes [17]. Because of its extremely precise surface area, nano-dimensional titanium dioxide allows for orderly charge separation and charge trapping of ions on its surfaces [18]. The oxidative power of the bulk-sized TiO_2 was found to rise with the opacity of the aqueous phase in the demonstration of nano-sized TiO_2 [19]. The aim of this work was prepared nanocatalyst by hydrothermal method and experimentations using response surface methodology by Minitab software to find organic removal in refinery wastewater (RWW) under different procedure variables by photocatalytic in two methods (TiO_2/UV, and ZnO/UV) and compare between them.

2. Experimental

2.1. Materials and organic test

Refinery wastewater polluted with organic droplets was obtained from the discharging of the Samawa oilfield refinery / South of Iraq and the specification is listed in Table 1. All materials used in this work were of analytical grade and secondhand deprived of any extra purification. The particle sizes of commercial titanium dioxide powder ≤40 nm were bought from India , zinc acetate , H_2SO_4 (SDFCL 98 % purity), and Sodium hydroxide (Thomas Baker). At end of each experiment 0.15 g of sodium chloride is added to 40 mL of RWW in the separating funnel after each experiment to break up the organic emulsion. Next, 5 mL of carbon tetrachloride is added and vigorously shaken for 2 min. After 25 min, the wastewater was separated into two layers, and the lower layer of oil was measuring using a UV-1800 spectro-photometer [20].

The organic elimination efficiency was assessed with Eq. 1:

$$\text{Organic removal} = \frac{C_\circ - C_t}{C_\circ} \times 100\% \quad (1)$$

2.2. Preparation of nano catalyst

To prepare a homogeneous solution of zinc oxide, 0.5 g of zinc acetate and 100 mL of distilled water were combined and stirred for 30 min without heating. Subsequently, the solution was transferred into a unique hydrothermal vial and heated to 200 °C for three hours (autoclave). After centrifuging the solution to create a pool, nanoparticles were analyzed by UV (absorption) analysis. Following the hydrothermal method's preparation, the substance was deposited using two different techniques: first, it was distilled onto glass substrates, and then it was spun. Three hydrothermally prepared samples were placed on glass substrates and dried for 30 min at 90 °C in an oven [21] with some modifications .

Table 1: Refinery wastewater properties.

Parameters	Values	Parameters	Values
Oil content	150.11 (ppm)	Conductivity	111442 (µs/cm)
Turbidity	48.5 NTU	TDS	71322.88 (mg/L)
pH	6.96	Viscosity	1.0404 (m Pa/S)
Solution oxygen content	0.062 (ppm)	Iron	0.44 (ppm)

2.3. Photocatalytic oxidation

A different dose of TiO_2 and ZnO of all the oxidation batch reactor of 250 mL was added to the wastewater solution for organic oxidation by free radical generation. Eight UV lamps with a wavelength of 365 nm and it was originated to be 0.5 mW/cm^2 to provide the UV light as present in Figure 1. The desired pH 3-9 was adjusted by using sodium hydroxide and sulfuric acid. 20-120 min was used for all the experiments.

2.4. Experimental design

In this work, the optimization of untried conditions aimed at refinery wastewater through a photocatalytic process remained presented through the Box Behnken design (BBD) method below RSM by the Minitab-17 program. The self-governing variables of oxidation time (X_1), catalyst concentration (X_2), and pH (X_3) as exposed in Table 2.

3. Results and Discussion

3.1. Characterization of photocatalyst

Figure 2 shows the FTIR spectral data that exposed the attendance of negatively charged functional groups (hydroxyl, carboxyl, and amine) on the surface of the nanocatalysts of TiO_2 and ZnO, with spectra in the range of 4000-500 cm^{-1}. The whole band at 3316.22 cm^{-1} in unadulterated bark powder remains accredited because of hydroxyl widening or amine stretching of polymeric complexes. The peaks of 1657.88 and 1369.44 cm^{-1} remain stating in the carbonyl group, 1259.12 cm^{-1} means the aromatic rings, though 1055.11 cm^{-1} remains related through the in phenols and the bands current underneath 822.23 cm^{-1} were fingerprint area of sulfur and phosphate functional groups [22]. It is cautious enough to leave an imprint regarding the presence of functional groups on the nano catalyst oxidant .

The surface morphologies of the nanocatalysts for TiO_2 and ZnO were observed by Fe-SEM analysis, as shown in Figures 3A and B, respectively. The way wastewater interacts with oxidants may have an impact on the morphologies of the materials used as nano-catalysts with range of nano particles in the range 40-90 nm with average 50 nm [23].

The XRD patterns of ZnO and TiO_2 nanoparticles that were produced are shown in Figure 4. With the same peaks observed for nanocatalysts, it validates the crystalline nature and hexagonal phase of ZnO and TiO_2. Using the Scherrer equation, the average crystallite size of ZnO nanoparticles is determined to be 30.33 nm by equation 2 [24]:

$$D = \frac{K\lambda}{\beta \cos\theta} \quad (2)$$

3.2. Statistical examination for photocatalytic

Table 3 explains the values of the operational variables and the responses of the final organic removal (OR) for each run.

Table 2: Working limits.

Limits	Varieties
X_1: reaction time (min)	20-120
X_2: catalyst dose (gm)	0.05-0.25
X_3:pH	3-9

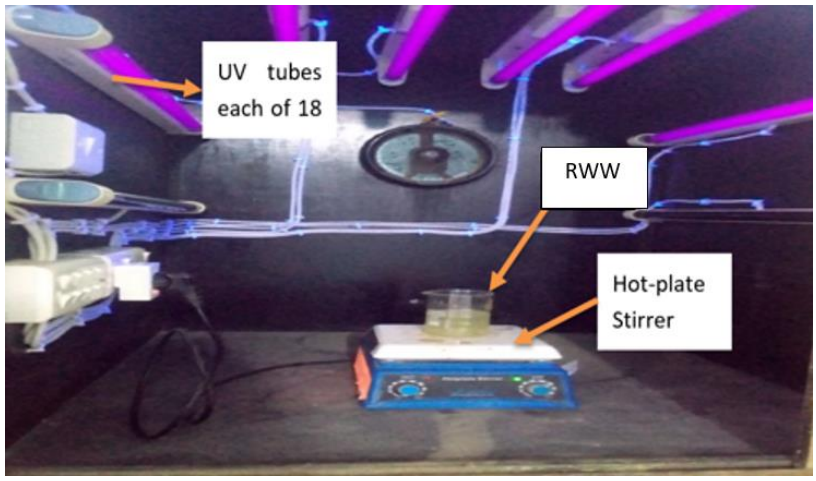

Figure 1: Photocatalytic oxidation.

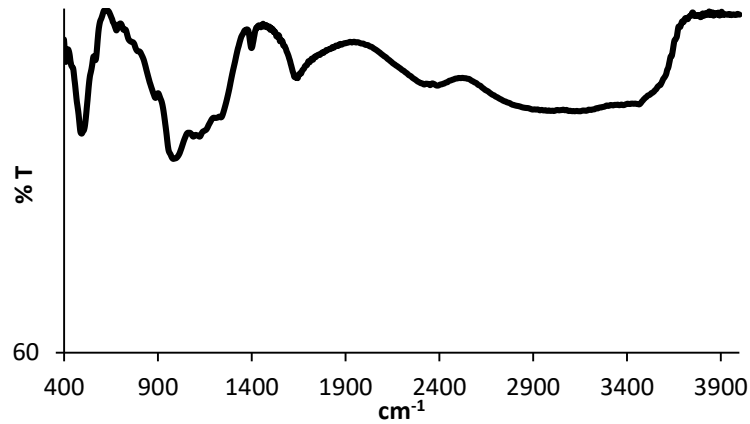

Figure 2: FTIR spectra of ZnO .

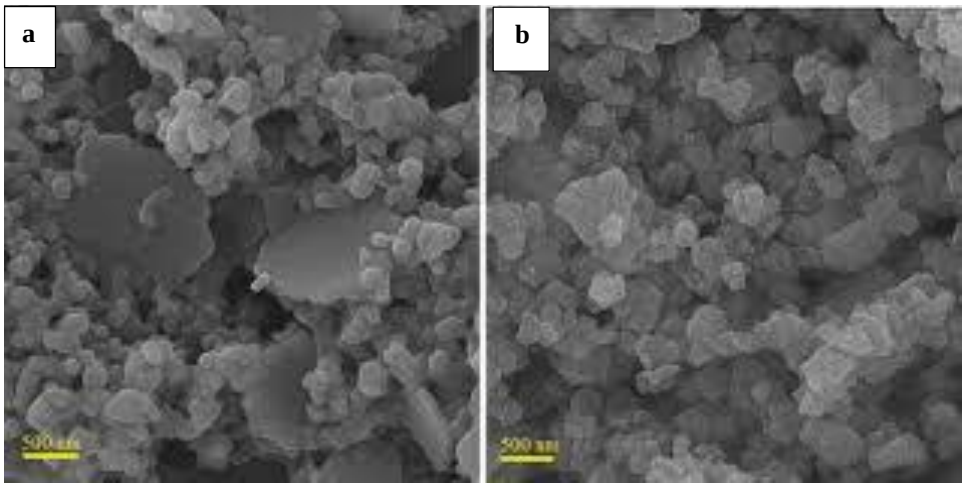

Figure 3: FE-SEM images of (a) TiO_2 and (b) ZnO.

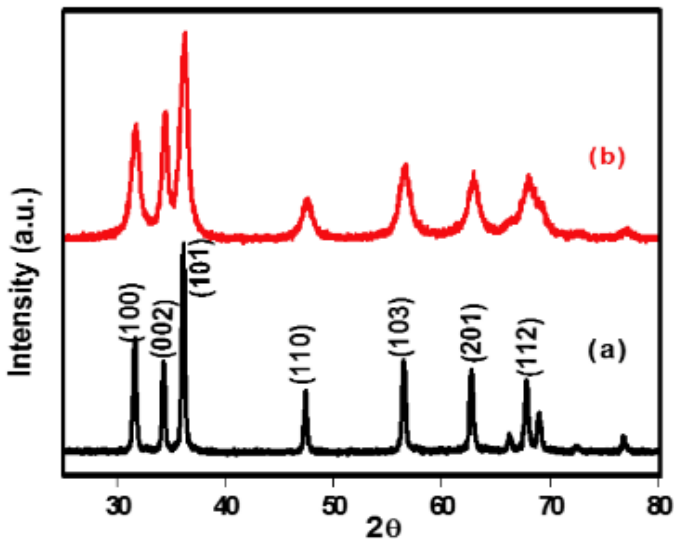

Figure 4: XRD pattern of (a) ZnO and (b) TiO_2.

Table 3: Results of BBD untried.

StdOrder	RunOrder	PtType	Blocks	Catalyst Dose (g)	pH	Irradiation time (min)	Organic removal by TiO_2	Organic removal by ZnO
1	1	2	1	0.05	3	70	34.523	41.25
2	2	2	1	0.2	3	70	67.28	72.45
3	3	2	1	0.05	9	70	68.28	75.89
4	4	2	1	0.2	9	70	91.28	93.89
5	5	2	1	0.05	6	20	47.622	55.28
6	6	2	1	0.2	6	20	72.45	80.2
7	7	2	1	0.05	6	120	62.48	68.15
8	8	2	1	0.2	6	120	77.89	84.77
9	9	2	1	0.125	3	20	55.811	66.28
10	10	2	1	0.125	9	20	75.26	80.28
11	11	2	1	0.125	3	120	52.89	60.89
12	12	2	1	0.125	9	120	88.28	91.82
13	13	0	1	0.125	6	70	76	82.5
14	14	0	1	0.125	6	70	76.89	83.02
15	15	0	1	0.125	6	70	75.89	82.88

Based on experimental results, the mathematical equations (Eqs. 3 and 4) were developed in terms of actual issues related to the oil removal to the operational variables revealing the interactions amid these variables :

$$\text{Organic elimination by } TiO_2 = -23.1 + 577.2\ X_1 + 9.5X_2 + 0.231X_3 - 1233\ X_1^2 - 0.443X_2^2 - 0.001686\ X_3^2 - 10.84\ X_1X_2 - 0.628\ X_1X_3 + 0.02657\ X_2X_3 \quad (3)$$

$$\text{Organic Removal by ZnO} = -14.9 + 603.5\ X_1 + 10.21\ X_2 - 0.512\ X_3 - 1302\ X_1^2 - 0.512X_2^2 - 0.001350\ X_3^2 - 14.67X_1X_2 - 0.553\ X_1X_3 + 0.02822\ X_2X_3 \quad (4)$$

The best model was affected by the ANOVA test Table 4 aimed at OR founded on the F test and P test. A regression equation resolves to show extra variance in response if the Fisher value is higher. BBD ability is documented by finished usage change parts done specific sources of alteration. The percent of model variability might be explained if the P-value was less than 0.05.

The conclusions are shown in Figure 5. The standards of positive coefficients demonstrated that cumulative factors related to these constants within the validated range improved the elimination efficacy. On the other hand, negative constant values showed that pH had a definite negative effect on OR. While the oxidation time and dose result in advantageous outcomes [25].

The primary assets of every limit on the OR are displayed in Figure 6 Dosage, pH, and time were the three variables that affected organic elimination in RWW the most. The positive value of this constant suggests that, for the variation under study, the cumulative dose and adsorption time would recover the OR. Furthermore, when this limit shifts from low to high, an increase in OR is shown, indicating that pH still has a substantial effect [26].

The percentage of organic removal for zinc oxide was above 93 %, whereas titanium dioxide was over 91 %. Figure 7 displays the optimal conditions for conducting experiments on ZnO photocatalytic systems, as determined using Minitab software.

Table 4: ANOVA for organic elimination for ZnO.

Foundation	DOF	Seq. SS	Adj. MS	F - Value	P– Value
1-Model	9	2789.14	309.90	39.78	0.000
Linear	3	2374.16	791.39	101.58	0.000
X_1	1	1029.22	1029.22	132.11	0.000
X_2	1	1275.38	1275.38	163.71	0.000
X_3	1	69.56	69.56	8.93	0.031
Square	3	282.54	282.54	12.09	0.010
X_1^2	1	198.05	198.05	25.42	0.004
X_2^2	1	78.34	78.34	10.06	0.025
X_3^2	1	42.09	42.09	5.40	0.068
2-Way Interaction	3	132.44	132.44	5.67	0.046
X_1*X_2	1	43.56	43.56	5.59	0.064
X_1*X_3	1	17.22	17.22	2.21	0.197
X_2*X_3	1	71.66	71.66	9.20	0.029
Error	5	38.95	7.79		
Lack-of-Fit	3	38.81	12.94	178.67	0.006
Pure ErroR	2	0.14	0.07		
Total	14	2828.809			

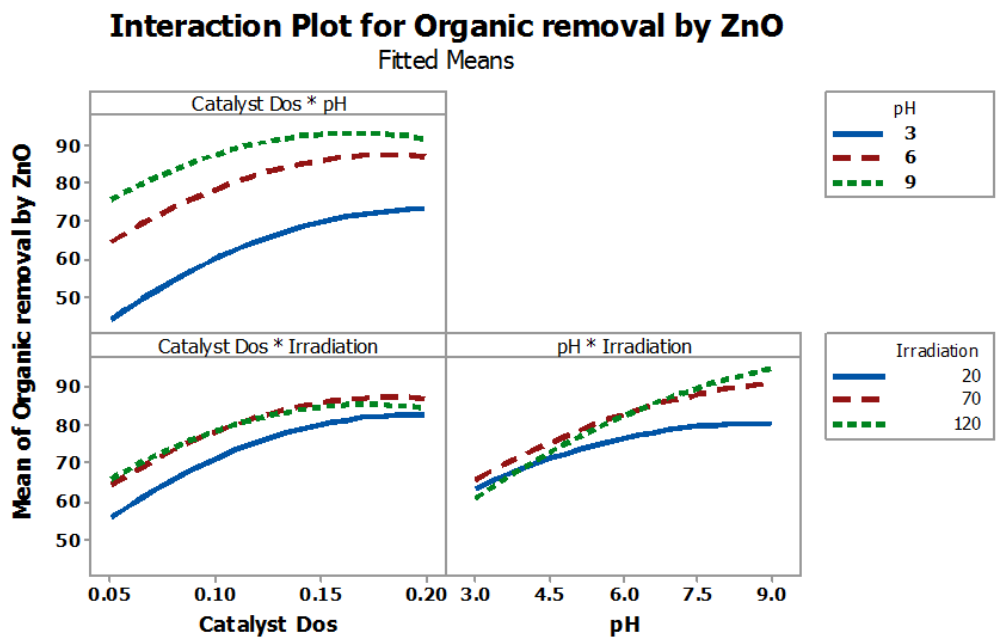

Figure 5: Interaction plot for organic removal.

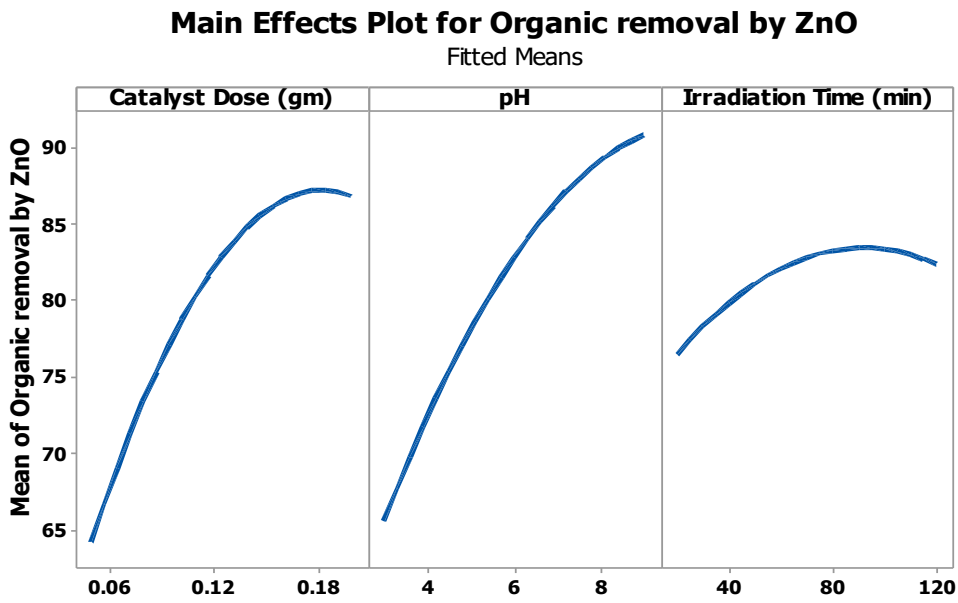

Figure 6: Main effects plot for oil removal.

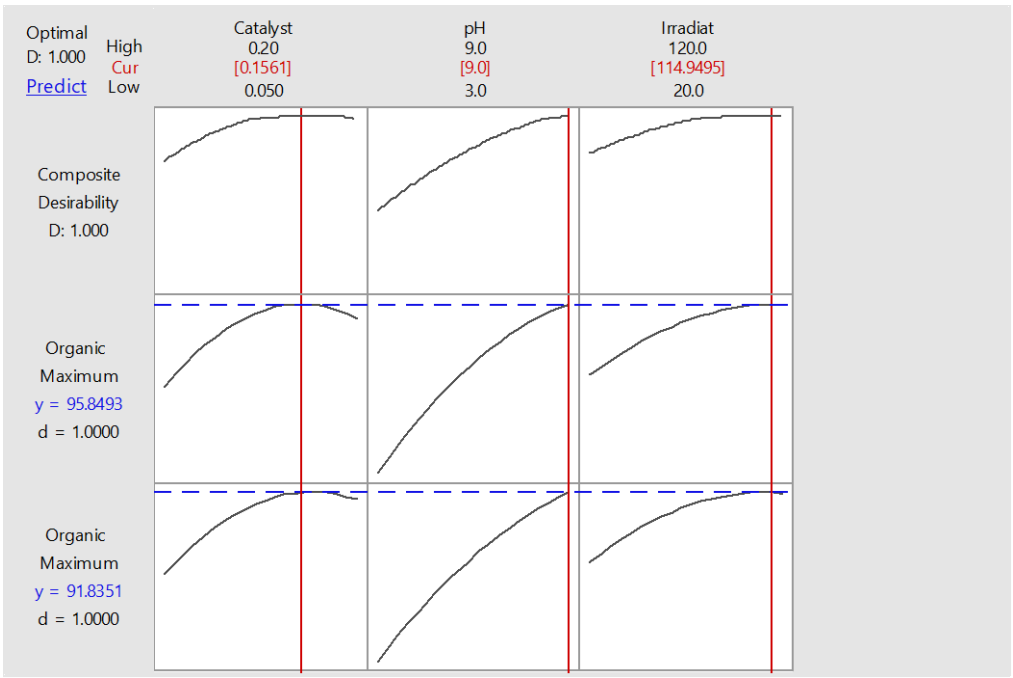

Figure 7: The best conditions of photocatalytic.

3.3. Effect of the photocatalytic dosage

The experimentations were shown below in two photocatalytic schemes; a-using TiO_2/UV and ZnO/ UV. Figure 8 demonstrates the result of the photo-catalytic on the recovery of organic from RWW. The organic elimination is augmented by way of the dose of catalyst dose augmented from 61.2 and 53.4 % at 0.05 g to the maximum elimination of 84.5 and 76.4 % at 0.2 g aimed at zinc oxide and titanium dioxide respectively. The highest amount of oxide agent has to be the result to evade the usage of the unnecessary catalyst in addition and also toward confirming the whole absorption of the photons so that an active catalytic remediation is reached. The upsurge in catalyst dose leads toward an upsurge in the catalyst surface area, therefore the elimination of the organic contaminants will be reduced [27].

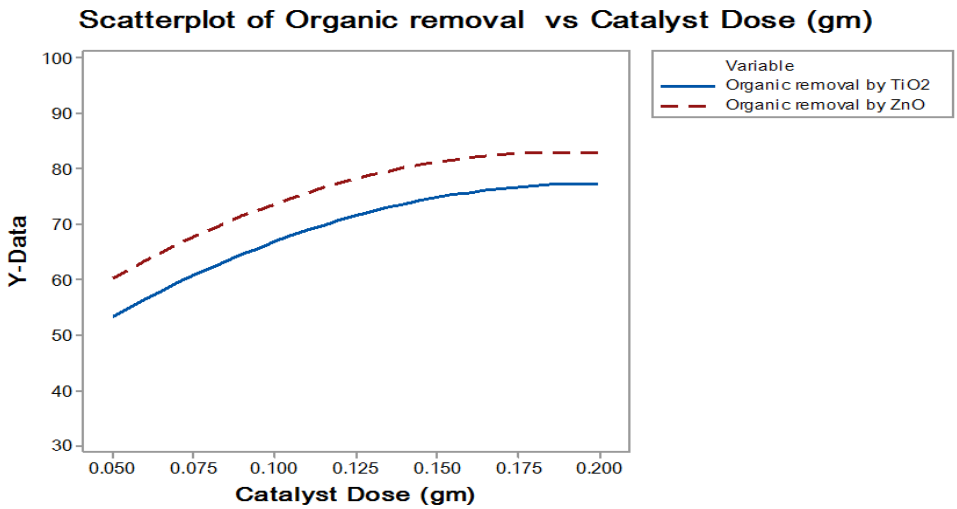

Figure 8: Effect of catalyst dose on organic elimination.

3.4. Effect of pH

The photocatalytic technique was meaningfully influenced through ended pH values then the finest presentation of the procedure demands a preferred pH diversity. Figure 9 displays the result of the pH of the solution on the recovery of organic in RWW. The driving forces of the advanced oxidation of the procedure were the active site of the catalyst and the manufacture of free radicals [28]. In an acidic medium, the charge of phot catalysis remains negative while it's a positive in an alkaline medium. pH meaningfully effects oil elimination from RWW through combined treatment using prepared nano catalyst by hydrothermal method [29]. The highest adsorption and oxidation efficiencies were observed at a pH of 9, indicating significant improvement in organic removal.

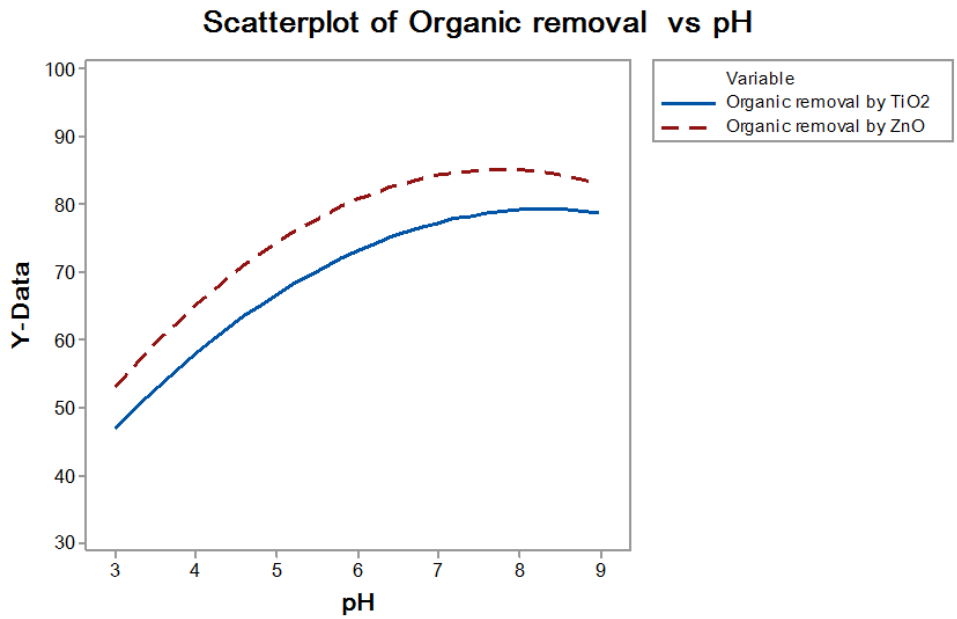

Figure 9: Effect of pH on organic elimination.

3.5. Effect of time on oil elimination

The inspection of oxidation time changeable aimed at the photocatalytic action and its importance on the organic removal in RWW was thoughtful. In the knowledge of photocatalytic, the free radicals produced, which need a high oxidizing capacity, can oxidize into rigidity with the failure of ions found in a little time. Figure 10 shows the relative between the organic removal and oxidation time along with the action development. Investigations have been shown to determine the premium time of oxidation competence in organic removal in refinery wastewater. The elimination of organic increased with the upsurge of time [30]. The increase in organic elimination can be connected to the photocatalytic of organic finished free radicals. The implication decided with previous studies that are obtainable is that the increase of oxidation time upsurges the competence of the method aimed at example that attained through Khalid et al. [31].

3.6. The mechanism of photocatalyst

The photo-degradation mechanism is described in Figure 11. The ZnO nanoparticles with band gap = 3.16 eV as shown in Figure 12 absorb photons greater than their band gap energy when UV light is event on them. Photo-induced electrons are then promoted from the valence band (VB) to the conduction band (CB), producing negatively charged electrons (e^-) and positively charged holes (h^+) on the surface of the zinc oxide. Because the dissolved oxygen in the water works as an electron scavenger, it produces reactive radicals ($O_2^{\cdot-}$), which in turn react with the water to form free radicals [32]. Because hydroxyl radicals are potent oxidants, they cause the organic matter to directly mineralize into carbon dioxide and water. Similar to this, holes and negatively charged hydroxyl ions combine to form free radicals, which aid in the breakdown of organic materials.

UV-Vis absorbance spectroscopy and photo-luminescence spectroscopy were used to ascertain the optical property of ZnO nanoparticles (Figure 12). ZnO has a significant absorption in the UV range of 200-395 nm, with an absorption edge at 410 nm, according to UV-Vis absorption spectra. The first-order model of oxidation is expressed as (Eq. 5):

$$\text{Ln}\ \frac{C_o}{C} = K_1 t \qquad (5)$$

A suitable correlation between oxidation time and the relation logarithm of the ratio of concentration initial and after treatment was found in the kinetics investigation for the synthesis of ZnO, as shown in Figure 13. This suggests with first order kinetic oxidation. When the pH is 9, the prepared nano material showed a constant rate value of 0.044 min^{-1}.

Table 5 differences the current work with preceding similar published papers, concentrating on untried features such as contaminant type, oxidation type and period, and the related degradation fractions. Particularly, the newly prepared composite solar-catalyst exhibits exceptional performance in comparison to previously documented conventional photo-catalysts. This comparison demonstrations the prepared material photo catalyst's superiority over currently obtainable conservative photo catalysts, in addition to its efficiency and potential for pollutant degradation under various testing conditions.

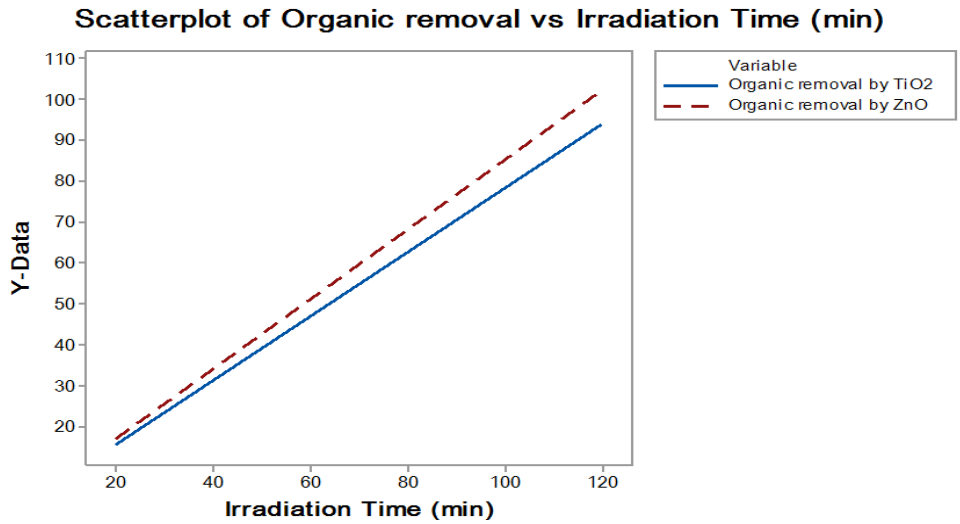

Figure 10: Effect of oxidation time on organic elimination.

Table 5: Comparison of the work with other works.

Treatment	Pollutants type	UV type	Period (min)	Degradation	Ref.
Zinc oxide	Phenol	UV	60	55.3%	[33]
Zinc oxide	Green dye	UV	60	92.8%	[34]
Titanium dioxide	dyes	UV	90	88%	[2]
Prepared ZnO	OP	UV	120	93.8%	This work

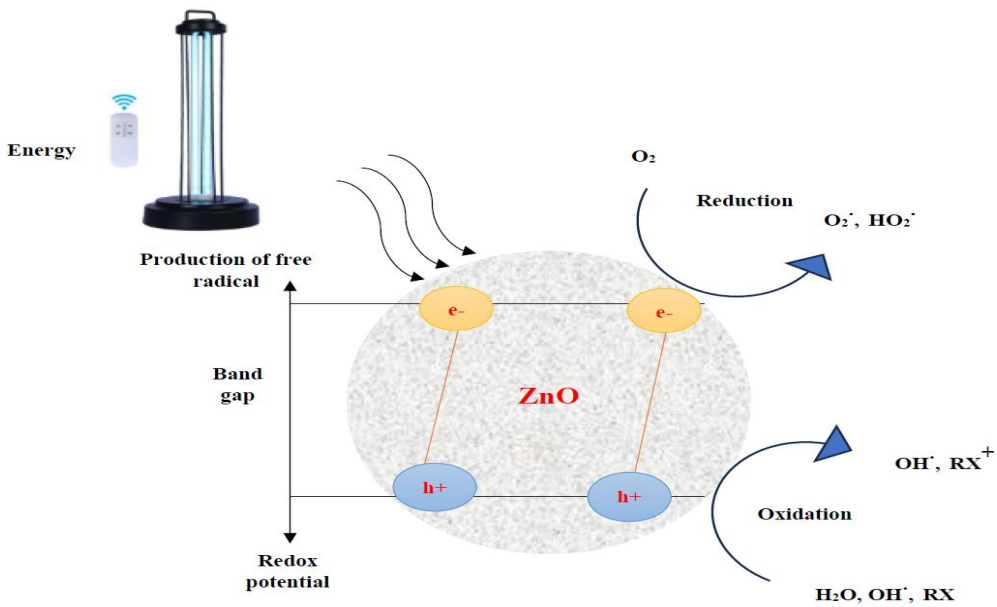

Figure 11: The Possible mechanism of photocatalytic degradation .

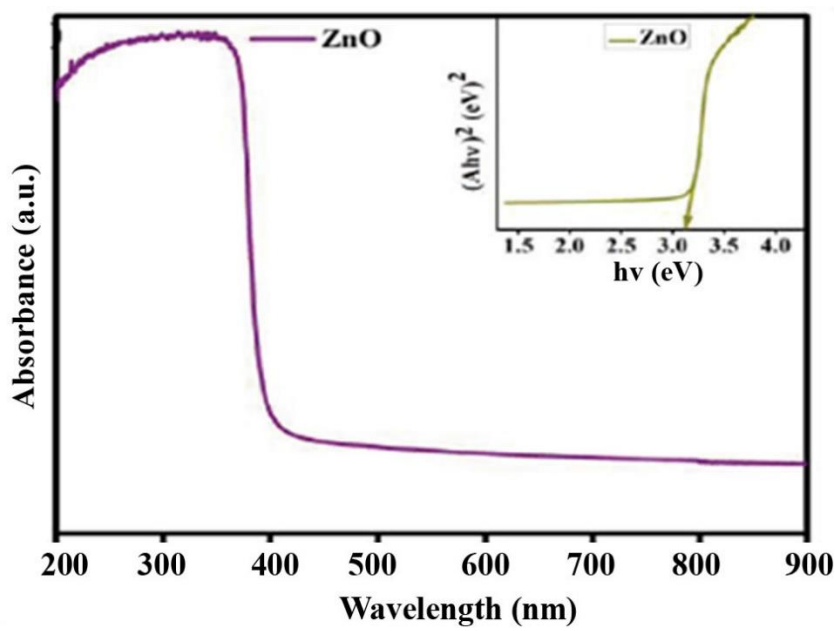

Figure 12: Diffuse reflectance spectroscopy of ZnO.

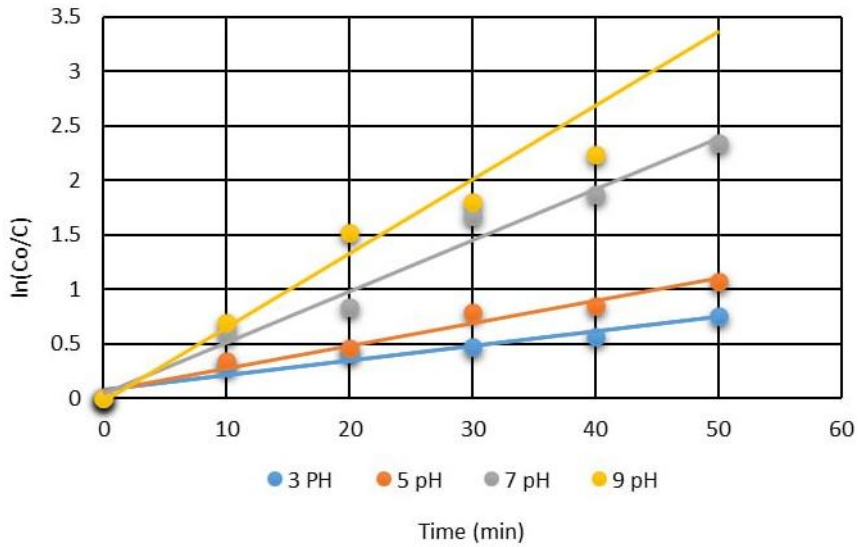

Figure 13: A plot of –ln (C/Co) vs. Time.

4. Conclusion

In conclusion, the synthesis of zinc oxide nanocatalysts via the hydrothermal method has proven to be an effective approach for enhancing the photocatalytic degradation of refinery wastewater. The optimized synthesis conditions led to the formation of high-quality ZnO nanoparticles with superior structural and optical properties. A refinery wastewater contaminated water with organic was subjected to a laboratory experimental study to show the competence of an advanced oxidation process toward removing the organic from polluted water using two systems: -UV/TiO_2, and UV/ZnO. Since the advanced oxidation process depends mostly on the amount of photo-catalytic, the pH of the solution, and the time of the process, the best of these conditions were applied for the above three systems. The results show that 93.89 and 91.28 % of the organic content in refinery wastewater was improved for zinc oxide and titanium dioxide correspondingly.

5. References

1. Ö. Kayan G, Kayan A. Composite of natural polymers and their adsorbent properties on the dyes and heavy metal ions. J Polym Environ. 2021; 29(11):3477-3496. https://doi.org/10.1007/s10924-021-02154-x.
2. Hassan AA, Al-Zobai KMM. Chemical oxidation for oil separation from oilfield produced water under UV irradiation using titanium dioxide as a nano-photo-catalyst by batch and continuous techniques. Int J Chem Eng. 2019; 2019:9810728. https://doi.org/10.1155/2019/9810728.
3. Sultan HK, Aziz HY, Maula BH, Hasan AA, Hatem WA. Evaluation of contaminated water treatment on the durability of steel piles. Adv Civ Eng. 2020; 2020:1269563. https://doi.org/10.1155/2020/1269563.
4. Jafer AS, Hassan AA, Naeem ZT. A study on the potential of Moringa seeds in adsorption of organic content from water collected from oilfield refinery. Pak J Biotechnol. 2019;16(1):27-33. https://doi.org/10.34016/pjbt.2019.16.1.5.
5. Al-Hassan AA, Shakir IK. Enhanced photocatalytic activity of CuO/NCW via adsorption optimization for refinery wastewater. Iran J Chem Chem Eng. 2024; In Press. https://doi.org/10.30492/ijcce.2024.2034599.6684.
6. Ibrahim MK, Al-Hassan AA, Naje AS. Utilisation of Cassia surattensis seeds as natural adsorbent for oil content removal in oilfield produced water. Pertanika J Sci Technol. 2019; 27(4):2123-2138. https://doi.org/10.5555/20219941435.
7. Hassan AA, Naeem HT, Hadi RT. A comparative study of chemical material additives on poly-acrylamide to treatment of waste water in refineries. IOP Conf Ser Mater Sci Eng. 2019; 518(6):062003. https://doi.org/10.1088/1757-899X/518/6/062003.
8. Nawaf AT, Hassan AA. Design of (MnO_2/GO) for removal organic compounds from wastewater using digital baffle batch reactor. Int J Environ Sci Technol. 2025; 1-20.10.1007/s13762-025-06414-4.
9. Hassan AA, Shakir IK. Kinetic insights into solar-assisted fabrication and photocatalytic performance of $CoWO_4$/NCW heterostructure. Bull Chem React Eng

Catal. 2024; In Press. https://doi.org/10.9767/bcrec.20198.
10. Alturki SF, Suwaed MS, Ghareeb A, AlJaberi FY, Hassan AA. Statistical analysis and optimization of mechanical-chemical electro-Fenton for organic contaminant degradation in refinery wastewater. J Eng Res. 2024;In Press. https://doi.org/10.1016/j. jer.2024.10.006.
11. Ohm TI, Cae JS, Zhang MY, Joo JC. Computational fluid dynamics modeling and field applications of non-powered hydraulic mixing in water treatment plants. Water. 2020;12(4):939. https://doi.org/10.3390/w12040939.
12. Saleh Jafer A, Hassan AA. Removal of oil content in oilfield produced water using chemically modified kiwi peels as efficient low-cost adsorbent. J Phys Conf Ser. 2019;1294(7). https://doi.org/10.3390/w12040939.
13. Zinatloo-Ajabshir S, et al. Novel rod-like $[Cu(phen)_2(OAc)]\cdot PF_6$ complex for high-performance visible-light-driven photocatalytic degradation of hazardous organic dyes: DFT approach, Hirshfeld and fingerprint plot analysis. J Environ Manage. 2024; 350:119545. https://doi.org/10.1016/j.jenvman.2023.119545.
14. Atiyah AS, Al-Samawi AAA, Hassan AA. Photovoltaic cell electro-Fenton oxidation for treatment oily wastewater. AIP Conf Proc. 2020; 2235. https://doi.org/10.1063/5.00089371.
15. Souza BM, et al. Removal of recalcitrant organic matter content in wastewater by means of AOPs aiming industrial water reuse. Environ Sci Pollut Res. 2016; 23(22):22947-22956. https://doi.org/10.1007/s11356-016-7476-5.
16. Orooji N, Takdastan A, Jalilzadeh Yengejeh R, Jorfi S, Davami AH. Photocatalytic degradation of 2,4-dichlorophenoxyacetic acid using Fe_3O_4@TiO_2/Cu_2O magnetic nanocomposite stabilized on granular activated carbon from aqueous solution. Res Chem Intermed. 2020; 46(5):2833-2857. https://doi.org/10.1007/s11356-016-7476-5.
17. Mohammadi Ziarani G, Rezakhani M, Feizi-Dehnayebi M, Nikolova S. Fumed-Si-Pr-Ald-Barb as a fluorescent chemosensor for the Hg^{2+} detection and $Cr_2O_7^{2-}$ ions: A combined experimental and computational perspective. Molecules. 2024; 29(20): 4825. https://doi.org/10.3390/molecules29204825.
18. Ulhaq I, Ahmad W, Ahmad I, Yaseen M, Ilyas M. TiO_2 supported CTAB modified bentonite for treatment of refinery wastewater through simultaneous photocatalytic oxidation and adsorption. J Water Process Eng. 2021;43:102239. https://doi.org/10.1016/j. jwpe.2021.102239.
19. Gutierrez-Mata AG, et al. Recent overview of solar photocatalysis and solar photo-Fenton processes for wastewater treatment. Int J Photoenergy. 2017; 2017:8528063. https://doi.org/10.1155/2017/8528063.
20. Mousa Al-Zobai KM, Hassan AA. Utilization of iron oxide nanoparticles (hematite) as adsorbent for removal of organic pollutants in refinery wastewater. Mater Sci Forum. 2022; In Press. https://doi.org/10.4028/p-i14w2f.
21. Strachowski T, et al. Hydrothermal synthesis of zinc oxide nanoparticles using different chemical reaction stimulation methods and their influence on process kinetics. Materials. 2022; 15(21):7661. https://doi.org/10.3390/ma15217661.
22. Humadi JI, Nawaf AT, Jarullah AT, Ahmed MA, Hameed SA, Mujtaba IM. Design of new nano-catalysts and digital basket reactor for oxidative desulfurization of fuel: Experiments and modelling. Chem Eng Res Des. 2023; 190:634-650. https://doi.org/10.1016/j.cherd.2022.12.043.
23. Civan G, Palas B, Ersöz G, Atalay S, Bavasso I, Palma LD. Experimental assessment of a hybrid process including adsorption/photo Fenton oxidation and microbial fuel cell for the removal of dicarboxylic acids from aqueous solution. J Photochem Photobiol A Chem. 2021; 407:113056. https://doi.org/10.1016/j.jphotochem.2020.113056.
24. Bushroa AR, Rahbari RG, Masjuki HH, Muhamad MR. Approximation of crystallite size and microstrain via XRD line broadening analysis in TiSiN thin films. Vacuum. 2012; 86(8):1107-1112. https://doi.org/10.1016/j.vacuum.2011.10.011.
25. Hassan AA, Shakir IK. Synthesis of nanocellulose using ultrasound-assisted acid hydrolysis for adsorption/oxidation of organic pollutants in wastewater under UV and solar light. J Sustain Sci Manag. 2024;19(12):120-140. https://doi.org/10.46754/jssm.2024.12.008.
26. Shahawy AE, Ahmed IA, Nasr M, Ragab AH, Al-Mhyawi SR, Elamin KM. Organic pollutants removal from olive mill wastewater using electrocoagulation process via Central Composite Design (CCD). Water. 2021; 13(24):3522. https://doi.org/10.3390/w13243522.
27. Atout H, et al. Integration of adsorption and photocatalytic degradation of methylene blue using TiO_2 supported on granular activated carbon. Arab J Sci Eng. 2017;42(4):1475-1486. https://doi.org/10.1007/s13369-016-2369-y.
28. Ahmed IH, Hassan AA, Sultan HK. Study of electro-Fenton oxidation for the removal of oil content in refinery wastewater. IOP Conf Ser Mater Sci Eng. 2021;1090(1):012005. https://doi.org/10.1088/1757-899X/1090/1/012005.
29. Li YY, Wu YL, Chen N, Ma YL, Ji WX, Sun YG. Preparation of metal oxide-loaded nickel foam adsorbents modified by biochar for the removal of cationic dyes from wastewater. Chin J Anal Chem. 2023; 51(8):100278. https://doi.org/10.1016/j.cjac.2023.100278.
30. Al-Khafaji RQ, Mohammed AHAK. Optimization of continuous electro-Fenton and photo electro-Fenton processes to treat Iraqi oilfield produced water using surface response methodology. IOP Conf Ser Mater Sci Eng. 2019; 518(6):062007. https://doi.org/10.1088/1757-899X/518/6/062007.

31. Al-zobai KMM, Hassan AA, Kariem NO. Removal of amoxicillin from polluted water using UV/TiO_2, UV/ZnO/TiO_2, and UV/ZnO. Solid State Technol. 2020;63(3):3567-3575.
32. Nawaf AT, Jarullah AT, Hameed SA, Mujtaba IM. Design of new activated carbon based adsorbents for improved desulfurization of heavy gas oil: experiments and kinetic modeling. Chem Prod Process Model. 2021; 16(3):229-249. https://doi.org/10.1515/cppm-2020-0107.
33. Aderibigbe FA, et al. Green synthesis of zinc oxide nanoparticles for the removal of phenol from textile wastewater. Discov Chem Eng. 2024; 4(1). https://doi.org/10.1007/s43938-024-00061-w.
34. Bedano NQ, Alkaim AF. Removal of pollutants from aqueous solutions by using zinc oxide nano-particles. Int J Pharm Qual Assur. 2022;13(3):275-279. https://doi.org/10.25258/ijpqa.13.3.09.

How to cite this article:
Hadi LT, Al-khateeb RT, Hassan AA. Synthesis of Zinc Oxide Nanocatalyst Via Hydrotherma Method for Photocatalytic Oxidation Process of Refinery Wastewater. Prog Color Colorants Coat 2025;18(4):479-491. https://doi.org/10.30509/pccc.2025. 167484.1368.